ELSEVIER

Biochimica et Biophysica Acta 1511 (2001) 156–167

BIOCHIMICA ET BIOPHYSICA ACTA
BBA

www.bba-direct.com

Molecular dynamics simulations of stratum corneum lipid models: fatty acids and cholesterol

Monika Höltje [a,c,*], Thomas Förster [b], Birte Brandt [c], Thomas Engels [b], Wolfgang von Rybinski [b], Hans-Dieter Höltje [c]

[a] *Jülich Research Center, IBI2, D-52425 Jülich, Germany*
[b] *Henkel KGaA, Henkelstr. 67, D-40191 Düsseldorf, Germany*
[c] *Heinrich-Heine-University, Institute of Pharmaceutical Chemistry, Universitätsstr. 1, Geb. 26.23, D-40225 Düsseldorf, Germany*

Received 27 June 2000; received in revised form 12 December 2000; accepted 3 January 2001

Abstract

We report the results of an investigation on stratum corneum lipids, which present the main barrier of the skin. Molecular dynamics simulations, thermal analysis and FTIR measurements were applied. The primary objective of this work was to study the effect of cholesterol on skin structure and dynamics. Two molecular models were constructed, a free fatty acid bilayer (stearic acid, palmitic acid) and a fatty acid/cholesterol mixture at a 1:1 molar ratio. Our simulations were performed at constant pressure and temperature on a nanosecond time scale. The resulting model structures were characterized by calculating surface areas per headgroup, conformational properties, atom densities and order parameters of the fatty acids. Analysis of the simulations indicates that the free fatty acid fraction of stratum corneum lipids stays in a highly ordered crystalline state at skin temperatures. The phase behavior is strongly influenced when cholesterol is added. Cholesterol smoothes the rigid phases of the fatty acids: the order of the hydrocarbon tails (mainly of the last eight bonds) is reduced, the area per molecule becomes larger, the fraction of *trans* dihedrals is lower and the hydrophobic thickness is reduced. The simulation results are in good agreement with our experimental data from FTIR analysis and NIR-FT Raman spectroscopy.

Keywords: Skin lipid; Molecular model; Palmitic acid; Cholesterol; Order parameter; Fourier transform infrared spectroscopy

1. Introduction

The human stratum corneum (SC) is the uppermost layer of the epidermis, consisting of flattened cells, the corneocytes, embedded in a mixture of lipids. The lipids of the SC are responsible for the barrier function of the skin. They act as a two-way barrier, i.e. protecting the body from water loss and from penetration of exogenous compounds.

SC lipids are arranged in broad, multilamellar sheets of organized bilayers. The bilayers consist of several different types of components, dominated by ceramides, cholesterol, and fatty acids, whereas phospholipids seem to be absent [1]. In this regard the composition of the lipid bilayers of the SC is unusual, since membrane bilayers mainly contain phospholipids.

In order to understand the complex nature of the SC lipid lamellae as well as the relationship between

* Corresponding author. Fax: +49-211-8113847;
E-mail: mhoeltje@pharm.uni-duesseldorf.de

0005-2736/01/$ – see front matter
PII: S0005-2736(01)00270-X

molecular composition and functionality, there have been many experimental investigations using small- and wide-angle X-ray diffraction [2,3], electron microscopy [4], infrared (IR) spectroscopy [5], nuclear magnetic resonance (NMR) techniques [6], and atomic force microscopy [7]. However, the results of these techniques, while being used very successfully to provide detailed atomic insights into protein structures, are often difficult to interpret in the case of lipid layers. This is due to the heterogeneity and semifluid character of lipid layers under physiological conditions.

Molecular dynamics (MD) simulations offer a tool to obtain an atomic scale picture of membrane structures that may assist the interpretation of experimental results. They have been used very successfully in recent years to study biomembrane systems in molecular detail (for detailed reviews see [8–10]).

We wanted to benefit from these studies, trying to transfer the approved methods, which have been used in the simulations of phospholipids, to SC lipids.

Skin lipids are complex mixtures of different types of molecules. There is some published work on MD simulations of mixtures. Beside the fundamental study of Egberts and Berendsen [11] on a system of sodium decanoate/decanol/water, we are aware of some recent studies in this field, one dealing with lauryl alcohol/laurate [12], all the others dealing with the interaction of cholesterol with phospholipids [13–17].

The present study focuses in particular on the influence of cholesterol on the short chain free fatty acid fraction of SC and is part of an ongoing project to develop a model of a SC lipid bilayer that may serve in understanding experimental results concerning the functions of the different skin lipids.

SC lipids are characterized by a very complex polymorphology with a plethora of chain melting transitions at different temperatures. Because the systematic construction of a 'complete' mixture of this complexity is not possible, we have chosen simple models as starting points. Those simplified skin barrier models have been used very successfully in numerous experiments testing skin permeability, toxicity, and barrier perturbing effects of a large variety of drugs and cosmetic formulations.

We started our calculations with the simulation of a pure fatty acid bilayer (model A). For this purpose we chose palmitic acid and stearic acid as representatives of the short chain fatty acids of the SC, since both substances are often used in experimentally investigated skin lipid models. Model B was formed by mixing the fatty acids with 50 wt% cholesterol. Model A was prepared to investigate the behavior of hydrated free fatty acids in a bilayer formation at skin temperature. Model B served us to determine the influence of cholesterol on a number of bilayer properties: areas per headgroup, conformations of the side chains (*trans* fraction), conformational order parameters (deuterium order parameters, S_{CD}), hydrocarbon thickness, and densities.

IR and Raman spectroscopy were employed to study chain melting and chain packing interactions of congruent mixtures. Simulation data were compared to the results of these experiments. We wish to emphasize that the goal of the present work was not to search for detailed quantitative descriptions of our model systems. The main reason for this was the lack of accurate experimental data on analogous mixtures on which our simulation results could be fitted. Rather it was our intention to provide a prediction of the overall qualitative properties of the skin lipid model systems.

2. Materials and methods

2.1. Initial structures

Molecule building was done with the aid of the program SYBYL6.4 (Tripos Inc., 1699 South Hanley Rd., St. Louis, MO 63144, USA). Starting from the crystal coordinates of stearic acid [18], we used the space group operations and the lattice transformations of the crystal to generate a monolayer of 141 fatty acid molecules. The molecules in the X-ray crystal structure are tilted and exhibit strong hydrogen bonds among the headgroups. We adjusted the coordinates so that all hydrocarbon chains were perpendicular to the layer plane and all of the polar headgroups were in the same plane to disrupt the crystal headgroup packing in order to save computational time. Two monolayers were used to construct a bilayer consisting of 282 molecules. 136 randomly chosen stearic acids (68 in each monolayer) were

changed to palmitic acid by removing the last two carbon atoms in the chain.

The fatty acids bilayer (model A) was transformed into model B by exchanging 112 (= about 50 wt%) of the free fatty acids randomly for cholesterol.

The models were put into rectangular boxes, with the z plane defining the direction of the bilayer normal. The boxes were then enlarged on both tops to receive water caps. The water content of SC is reported to be very low (about 10 wt%) [19]. Simulations with a number of water molecules according to this value gave unstable runs, since the very small hydration level of about 2.5 water molecules per fatty acid led to insufficient solvation of the headgroups in the boundary region. Thus we increased the water content to 26 wt%: 1515 H_2O in model A and 1707 H_2O in model B. The chemical formulas of the compounds are shown in Fig. 1. Fig. 2 is a schematic diagram of one bilayer surface of model B, illustrating the positions of the cholesterol molecules among the fatty acids.

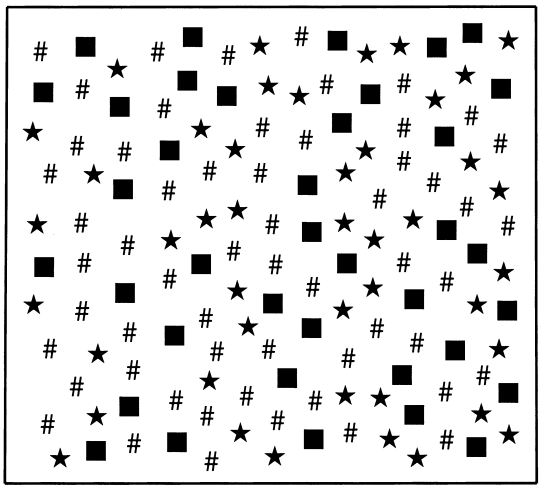

Fig. 2. Schematic diagram of the surface of model B showing the placing of cholesterol among the fatty acids: # cholesterol (50 wt%), ■ palmitic acid (22 wt%), ★ stearic acid (28 wt%).

2.2. Force field

Standard parameters of the GROMOS87 force field [20] were used with increased repulsion between water oxygen and carbon. Explicit atoms and hydrogens were used for all polar groups, whereas united atoms were used for the hydrocarbons. For the CH_2 and CH_3 groups of the fatty acids the Ryckaert–Bellemans potentials were applied, which appear to be well suited for membrane simulations, since they yielded experimentally observed *trans*/*gauche* ratios for hydrocarbon chains in phospholipids [21]. For water we employed the SPC model. Both the bond lengths and the bond angles in the water molecules were constrained by the SETTLE algorithm [22].

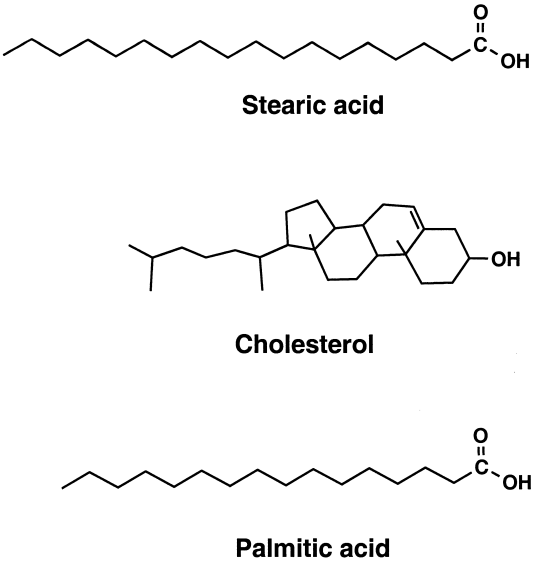

Fig. 1. Structures of the molecules used in the simulations.

2.3. Electrostatics and cutoff corrections

Point charges for the polar headgroups were derived from adequate GROMOS topology blocks. In human skin a pH gradient is found, reaching from pH 7 in the innermost SC layers to a pH of about 5 on the SC surface. Thus moving outwards, across the SC, the degree of ionization will drop from 90% to less than 10% at pH 5 [23]. Since we are interested in the SC surface, we used neutral fatty acids and no corresponding soaps in the present study.

A group based twin range cutoff of 1 nm/1.8 nm was applied. Up to 1 nm all atom pair interactions were calculated, between 1 nm and 1.8 nm only electrostatic interactions were taken into account.

2.4. Simulation conditions

All simulations were done with GROMACS [24]

on a SGI Indigo2 or a SGI Origin 2000 (Silicon Graphics, Mountain View, CA, USA).

The initial molecular geometry of the bilayers together with the water caps was first optimized with a conjugate gradient method. Periodic boundary conditions were applied in all three dimensions, so that actually a multilamellar system was represented, similar to that found in the SC.

Simulations were performed with weak coupling to a bath of constant temperature, with a coupling time $\tau = 0.1$ ps. Fatty acids, cholesterol, and water molecules were coupled individually to the heat bath. Isotropic pressure coupling was applied with a coupling constant $\tau = 0.1$ ps at 1 bar. A time step of 1 fs was used without any constraints on the molecules.

It is well known that membrane simulations starting with phospholipids in the well ordered and closely packed crystal lattice can require very long equilibration times and reminiscences of the primary ordering can be still seen in the final structures even with simulations up to several hundreds of picoseconds at physiological temperatures, a finding that agrees well with our own simulation experience on model A. Thus we used a simulated annealing procedure to disrupt the crystal packing of model A during the high temperature phase followed by a cooling down to skin temperature thus allowing the system to adjust its volume and shape and to find its adequate size.

First a 200 ps MD run was performed at 350 K, a temperature which is above the melting temperature of palmitic acid (63°C) and stearic acid (69.6°C). Then the temperature was gradually lowered to 303 K. After this temperature was reached, simulations were carried out at constant temperature for several nanoseconds. The initial structure of model B was constructed from a gel phase ensemble taken from the simulation of model A at 350 K.

2.5. Preparation of model mixtures

Fatty acids and, if indicated, cholesterol (all from Sigma Chemie, Deisenhofen, Germany) were mixed with distilled water, heated to 70°C in a glass beaker and stored at this temperature for 2 days to reach equilibrium. Then the samples were cooled to room temperature and stored for at least another 2 days.

2.6. Fourier transform infrared (FTIR) data

The model mixtures were melted at 323 K, pressed between Si/KBr plates and filled into an electrical heating cuvette (Perkin Elmer). At 300 K, 310 K, and 333 K IR spectra were taken. The spectra were acquired with a Bruker IFS88 spectrometer equipped with a DTGS detector (Bruker, Karlsruhe, Germany). The IR spectra were collected from 32 interferograms at 2 cm^{1-} resolution. Accuracy of the temperature control is about ± 5°C. The mentioned frequencies are mean values of two measurements.

2.7. Near infrared Fourier transform (NIR-FT) Raman spectroscopy

The Raman measurements were made with the Bruker (Karlsruhe, Germany) Raman spectrometer RFS 100. The 1064 nm line with 300 mW from a Nd:YAG laser was used as the excitation source. A liquid nitrogen cooled Ge detector was used.

3. Results

3.1. Area per molecule and trans fraction

The surface area per molecule is represented by the cross-sectional area available to each molecule at the bilayer–water interface. It was calculated by dividing the *xy* surface area of the simulation box by the number of molecules in one layer.

In Fig. 3a we show the average area per fatty acid of model A as a function of time. During the 200 ps high temperature run, the area per headgroup increased from 20 $Å^2$ to 24 $Å^2$ because the initial highly ordered crystal arrangement is destroyed. Connected with this a disordering within the alkyl chains begins indicated by the formation of *gauche* conformers, as can be seen from the run of the *trans* fraction in Fig. 3b. The number of *trans* bonds decreased to a value of about 80%. When the system is cooled down to skin temperature (303 K), the fatty acids start to rearrange into an ordered ensemble again. The area per headgroup moves continuously to smaller values and the *trans* fraction increases again. This process had not reached equilibrium after 2600 ps, but since the tendency can be seen very

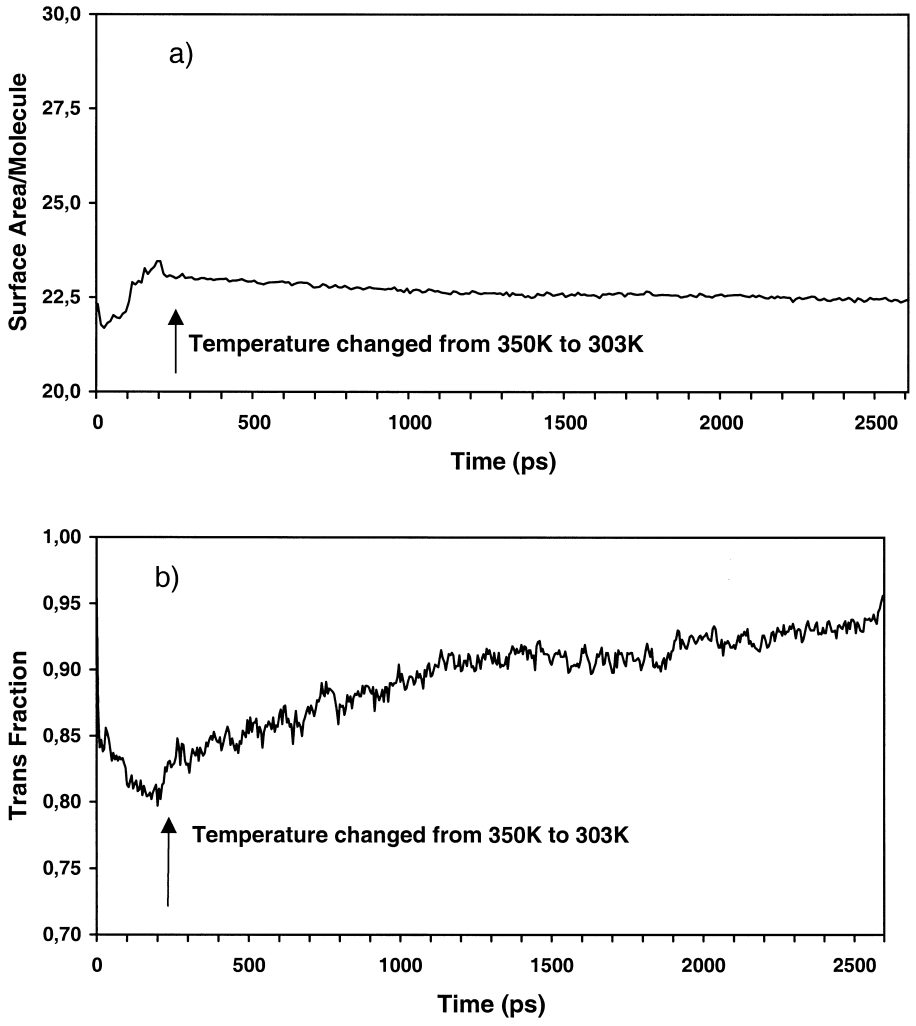

Fig. 3. (a) Time evolution of the surface area per molecule of model A. (b) *Trans* fraction development of the hydrocarbon chains of model A.

clearly, we stopped the simulation at the point where the *trans* fraction achieved 0.95 again and the area per headgroup obtained a value of 22 Å^2. The structural changes of model A during the simulation can be seen nicely from Fig. 4a,b, which shows a cross-section through the bilayer at two different time steps (200 and 2600 ps). Starting from fully extended crystalline hydrocarbon chains, which were arranged perpendicularly, the bilayer reached a premelting phase during the high temperature run (Fig. 4a). Cooling down results in highly ordered chains again, which now exhibit a strong tilt to the bilayer plane (Fig. 4b), a formation that looks similar to a L_{β}' gel phase in which the polar head groups are disordered but the mostly all-*trans* chains are packed regularly in a tilted manner.

The resulting molecular arrangement of model B is presented in Fig. 4c,d. It is seen that the hydrocarbon chains are partly disordered. These chains have a substantial gradient away from the bilayer normal, but in contrast to Fig. 4b there is no collective tilt of the whole assembly of chains.

Fig. 5a shows the time dependent development of the average area per molecule in model B and Fig. 5b the corresponding *trans* fraction of the alkyl chains. Since in the starting structure of model B the fatty acids are already in premelting conformations, no high temperature run was necessary. The total simulation was performed at 303 K. From the start, the *trans* fraction oscillates around 0.8 and converges to a value of 0.81 for the last 500 ps. No upward tendency can be seen, a result which is quite in contrast

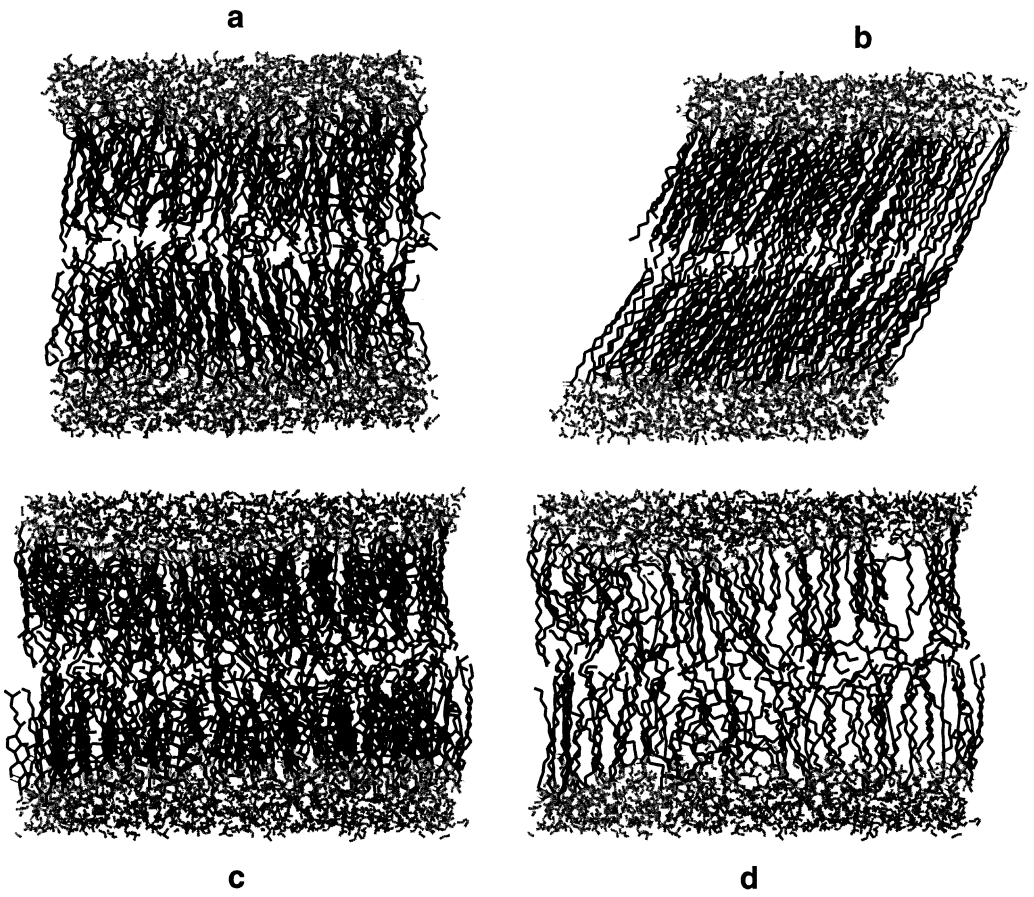

Fig. 4. Snapshots of the simulation models. Water molecules are shown in gray, fatty acids and cholesterols in black. (a) Model A at the end of the high temperature run, and (b) at the end of the simulation (2600 ps). (c) Model B at the end of the simulation, and (d) like (c) with cholesterol molecules removed to show the conformations of the fatty acids.

to model A. Thus, the results suggest that when the fatty acids are mixed with cholesterol, they reach a stable conformational state during the simulation time. To characterize that state we wanted to compare our *trans* fractions with data from investigations on dipalmitoylphosphatidylcholine (DPPC), one of the most studied lipids. Experimental results for the liquid crystalline L_α phase of DPPC demonstrate *trans* fractions of 0.76–0.6, depending on the method used [25–27]. For the L_β phase a *trans* fraction of above 0.9 has been derived from Raman measurements as well as from MD simulations [15,27]. Thus the *trans* fraction in our model B simulation lies between the values of a gel and a liquid crystalline phase.

The time evolution of the average surface area per molecule converged very rapidly in model B as can be seen from Fig. 5a. During the first simulation steps the surface area decreased, since the placement of the cholesterol molecules led to a somewhat loose starting arrangement. After $\sim$50 ps the surface area had dropped to a value of about 29 Å^2 and it remained stable for the remaining run.

In model A we obtained an area per fatty acid molecule of $\sim$24 Å^2 when the *trans* fraction reached 80%. Assuming that the area per fatty acid has not changed in model B, since the *trans* fraction is likewise 80%, we get an estimate for the area per cholesterol molecule by subtracting from the total area per monolayer the total average area occupied by the fatty acid molecules (141×24) and dividing the difference by the number of cholesterols per monolayer. We calculate an average surface area of 35 Å^2 for the cholesterol in model B. This value is 4 Å^2 smaller than the value obtained by Hyslop et al. [28] in a cholesterol monolayer and 2.5 Å^2 larger than the values

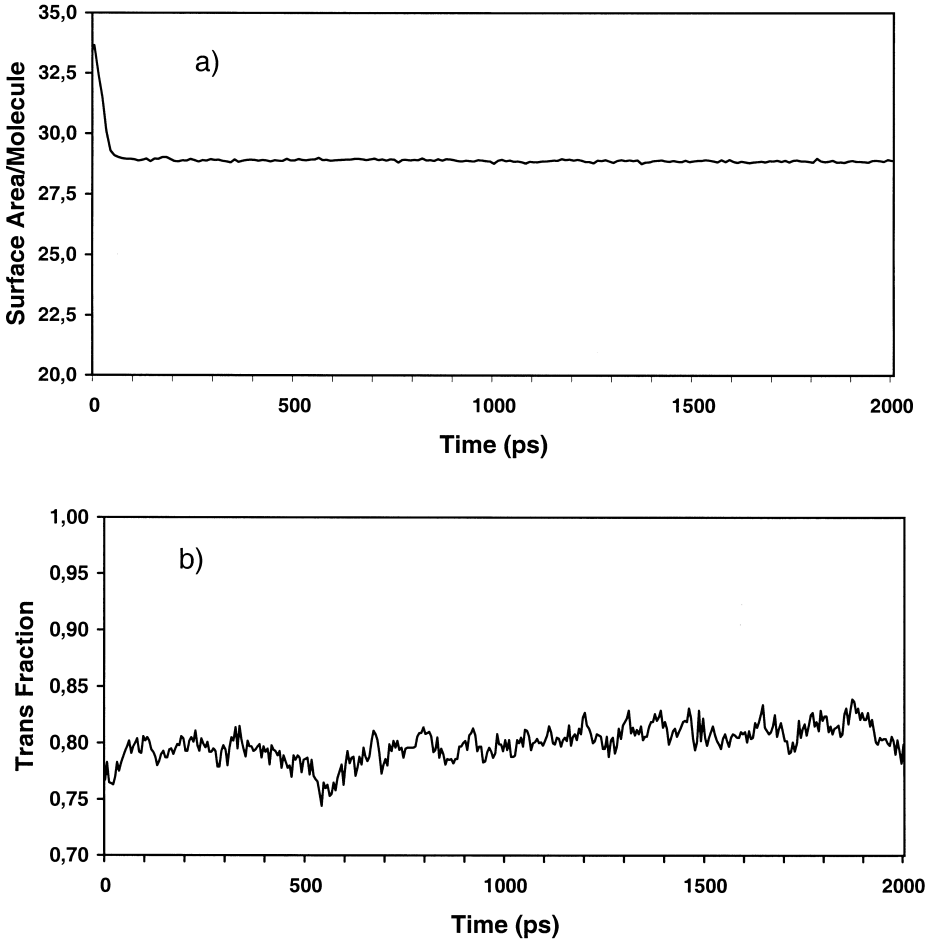

Fig. 5. (a) Time evolution of the surface area per molecule of model B. (b) *Trans* fraction development of the hydrocarbon chains of model B.

used by Tu et al. [15] and by Smondyrev et al. [16] in their simulations on DPPC/cholesterol mixtures.

MD calculations which we performed on a pure cholesterol bilayer resulted in an area per cholesterol of 37 Å^2. We interpret the divergence in the overall data as follows: in pure cholesterol ensembles, the rigid molecules exhibit highly hindered motions which do not allow much closer contact than in a crystal (about 39 Å^2). When single cholesterol molecules are surrounded by flexible and pliant hydrocarbon chains a much closer arrangement is possible, reducing the surface area to smaller values (e.g. down to 32 Å^2). Thus a value of $\sim$35 Å^2 for our model B seems to be reasonable, since not all cholesterol molecules are isolated and cholesterol–cholesterol contacts are to be found in the ensemble.

3.2. Deuterium order parameter (S_{CD})

Order parameters characterize the orientational order of the hydrocarbon chains and can be measured using the NMR technique. In MD simulations the deuterium order parameter (S_{CD}) can be calculated for each carbon in a chain using the following expression [11]:

$$S_{CD} = (2/3\cos^2\Theta - 1/2) \quad (1)$$

where Θ is the angle between the ith molecular axis and the bilayer normal (z axis).

Fig. 6 shows the calculated S_{CD} values of the palmitic acids in models A and B. The curves are plotted as a function of the carbon position along the chain (the carbon atom next to the carbonyl group is

designated number 1, the terminal methyl group is not calculated).

Let us first examine the order parameter profile of model A at the end of the high temperature run. The S_{CD} values remain practically constant along the central region (carbons 4–8) and drop slightly towards the beginning and the end of the carbon tail. The increased order of the alkyl chains, which occurred when the temperature was reduced to skin values, can be clearly seen from the profile which results from the end of the simulation. All carbon atoms now exhibit very similar order parameters. In spite of the increased conformational order within the chains, the average S_{CD} values have decreased (from 0.29 to 0.25). This just reflects the fact that the hydrocarbon chains are now tilted and their overall orientation is no longer parallel to the bilayer normal.

The experimental studies available for comparable fatty acids offer average S_{CD} values of soaps ranging from 0.19 to 0.14 at room temperature [29]. Soaps, due to their strong headgroup repulsion and hydration, need larger areas per molecule than neutral fatty acids. This obviously leads to a looser molecular packing in the hydrocarbon region and an increased conformational flexibility of the chains as can be seen from the low average S_{CD} values. The third profile in Fig. 6 demonstrates the effect of cholesterol on the alkyl chains. As can be seen, influences on the order of the palmitic acids are not uniform

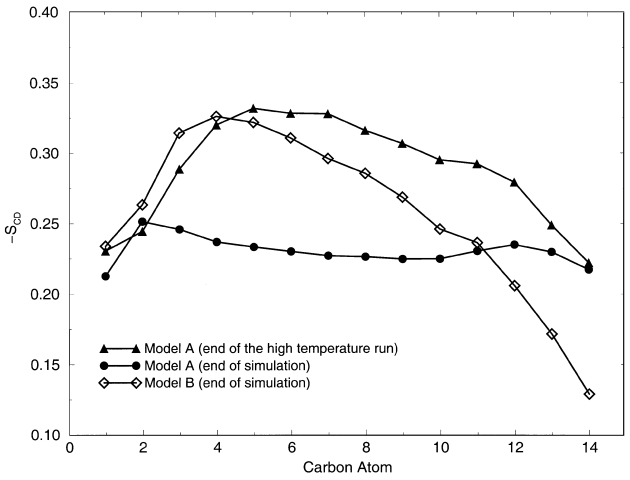

Fig. 6. The calculated deuterium order parameters S_{CD} of the palmitic acid chains as a function of carbon atom position in model A and model B.

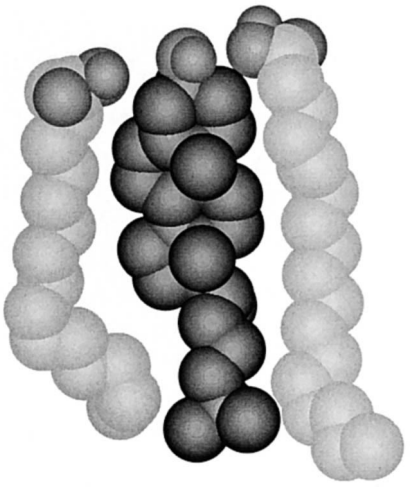

Fig. 7. Example of a typical cholesterol–fatty acid ensemble. Cholesterol is drawn in black, the hydrocarbon chains of palmitic acid (left) and stearic acid (right) are in gray.

along the hydrocarbon chains. There is little effect on the order parameters of the first carbon atoms, these values are only slightly higher in model B than in model A. The profile shows only a small plateau region extending over carbon atoms 3–6, after which the values drop significantly towards the end of the chains. It is apparent from the data that cholesterol induces a strong decrease in conformational order at the tail ends of the fatty acids, thus producing an order profile with the general features observed for phospholipid bilayers in the liquid crystalline phase (a plateau region near the carbonyls, followed by a decrease in order to near zero at the terminal methyl). The average S_{CD} values of both models do not differ so much (0.29/0.25 for model A and 0.26 for model B), whereas the appearance of the profiles is well defined. The experimentally well known effect of cholesterol to disorder lipid chains in gel phase bilayers can be clearly seen from the order parameters. In order to have a closer look at this effect, we present a representative set of molecules extracted from our simulations in Fig. 7. It is clear from the picture why cholesterol has such a profound effect on the conformation of the alkyl chains at the tail ends. For fatty acids neighboring cholesterol, the upper half of the chains is in contact with the rigid steroid ring, which reduces the conformational freedom, whereas the lower part is mainly in contact with the skinnier and more flexible cholesterol tail, which allows kinks in that part of the chains.

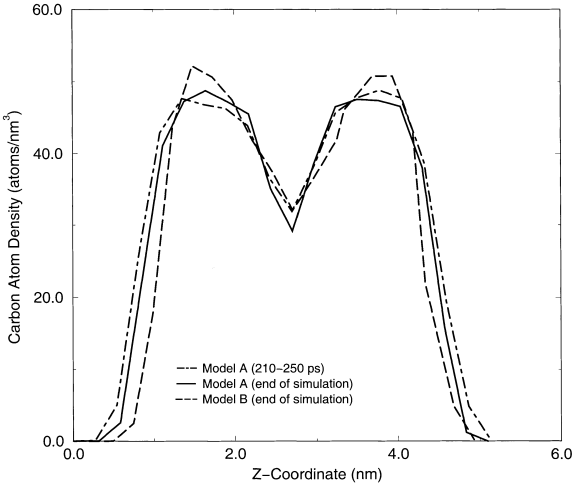

Fig. 8. Carbon atom density profiles along the bilayer normal of model A and model B averaged over 50 ps.

3.3. Hydrocarbon thickness and density

Looking at Fig. 4 again, an additional observation can be made: it is visually apparent from comparison of the ensembles that the thickness of the alkyl chain area along the bilayer normal is different in the two models. These findings are complemented by atom density calculations shown in Fig. 8. All profiles show a characteristic minimum in the center of the bilayer and a maximum in the middle of each monolayer. We can see that differences among the model A data plotted from the beginning and the end of the 303 K run are very small. The addition of cholesterol in model B results in a spreading and an increase of the density peaks. Thus the thickness of the hydrocarbon area is decreased and the atom density is increased through the presence of cholesterol.

We have calculated the thickness of the hydrocarbon region (H) in the bilayer with the formula [30]:

$$H = \langle ; |\overline{Z}_1(C_{carb}) - \overline{Z}_2(C_{carb})| \rangle \quad (2)$$

where $\langle\rangle$ denotes averaging over simulation time, $Z(C_{carb})$ is the z coordinate of the carbonyl carbon atom. $\overline{Z}$ is calculated by averaging all carbonyl carbon atoms in one monolayer. Z_1 is for the first monolayer and Z_2 for its opposing monolayer. Using this formula we get $H = 36.2$ for model A for the first 50 ps of the 303 K run and $H = 35.0$ for the last 50 ps. The decrease in H clearly is due to the collective tilt of the chains which had occurred at the end of the simulation. The calculated hydrocarbon thickness for model B is $H = 33.1$. Thus cholesterol leads to a reduction of the bilayer thickness in our simulations. As we have already seen, this effect can be explained by an increased number of *gauche* conformations and a decreased chain order which allows the fatty acids to bend around the cholesterol molecules and which subsequently leads to an decrease in bilayer width.

3.4. Experimental results on model SC mixtures

The MD simulation study reveals a strong influence of cholesterol on the *trans*/*gauche* fraction and order parameters of the alkyl chains of the fatty acids. Therefore, we decided to compare the theoretical results with experimental data from FTIR analysis of mixtures A and B, to detect phase change behavior. The exact frequency positions of the CH_2 stretching vibrations in the range from 2950 cm^{-1} to 2800 cm^{-1} change sensitively with the fraction of *trans*/*gauche* conformations in the alkyl chains of the fatty acids. An increasing *gauche* fraction results in a shift to higher wavenumbers.

In addition, we investigated both mixtures by NIR-FT Raman spectroscopy to get experimental insights into the conformational order of the alkyl chains as a function of temperature. From the ratio of the band heights for the symmetric CH stretching modes at 2890 cm^1 and 2850 cm^1 the order parameter for the lateral interaction S_{lat} is calculated [31]:

$$S_{lat} = (I_{2890}/I_{2850} - 0.7)/1.5 \quad (3)$$

S_{lat} indicates the packing order of the alkyl chains. It changes from 0 for the liquid state to 1 for the crystalline state.

The resulting data are shown in Table 1. By increasing the temperature from 300 to 333 K, the symmetrical CH_2 stretching frequency of model A compounds is shifted from 2848.1 cm^{-1} to the slightly higher value of 2848.6 cm^{-1}, indicating a higher fraction of *gauche* conformations. It is remarkable that the same frequency (2848.6 cm^{-1}) is already obtained at 300 K, when cholesterol is added to the pure fatty acids (model B).

This fluidizing effect of cholesterol is also observed from the Raman spectra. The evaluation of the lateral order parameter S_{lat} shows a distinct reduction in lipid packing order for model B compared to the

Table 1
IR and Raman data on model lipid mixtures

	Mixture A	Mixture B
Stearic acid (wt%)	16.76	8.40
Palmitic acid (wt%)	57.20	28.86
Cholesterol (wt%)	0	36.96
Water (wt%)	26.04	25.78
CH_{2sym} cm^{-1} at 300 K	2848.1	2848.6
CH_{2sym} cm^{-1} at 310 K	2848.3	2848.7
CH_{2sym} cm^{-1} at 333 K	2848.6	2849.1
Alkyl chain order parameter S_{lat} at 300 K	0.66	0.40
Alkyl chain order parameter S_{lat} at 310 K	0.63	0.32
Alkyl chain order parameter S_{lat} at 318 K	0.59	0.16

pure fatty acid mixture. It can be seen from Table 1, that the S_{lat} values of mixture A decrease only slightly from 0.66 to 0.59 during the temperature increase. In contrast, mixture B has smaller values and there is a significant difference between the values: the temperature increase from 300 K to 318 K reduces the S_{lat} value from 0.40 to 0.16.

It is interesting to compare these experimental in vitro results from model mixtures to real human lipid mixtures from ex vivo skin biopsies. Gay et al. [32] found that human SC lipids change their CH_2 stretching frequency from 2849.7 cm^{-1} to only 2850.8 cm^{-1} in the temperature range from 298 K to 333 K. This correlates well with the small frequency shift seen in the fatty acid/cholesterol/water mixture of model B. Even the absolute wavenumbers are close together.

4. Discussion

The behavior of the fatty acids in the MD simulations is in good agreement with the experimental data from our laboratory as well as from the literature. Neubert et al. [33] carried out FT Raman analyses of the melting behavior of stearic acid and found that in a double layered subcell the highly ordered all-*trans* structure of the alkyl chains was present up to about 5°C below the melting point. Between 65°C and the melting point *gauche* bonds appeared among *trans* sequences. On melting the lamellar arrangement disappeared and the resulting structure was a random mixture of *gauche* and *trans* bonds. Bearing these results in mind we interpret our simulation data as follows: within the 200 ps run at 350 K the fatty acids reach the premelting phase, the area per molecule and the number of *gauche* bonds increase by 20%. Cooling after 200 ps to skin temperature stops the melting and the fatty acids slowly revert to a highly ordered state.

The well ordered arrangement of the pure fatty acids is shifted to less rigid conformations when cholesterol is added. This fluidizing effect of cholesterol is well known and can also be recognized from our experimental data. But we should note that the chains are not fully fluidized (in contrast to liquid crystalline membrane bilayers), because the resulting *trans* fraction of 0.8 is too low to indicate an L_α phase. Experiments done on SC lipids showed similar results. The authors found in SC lipids at skin temperature orthorhombic phases with alkyl chains in the predominantly all-*trans* conformation when no cholesterol was present and hexagonal phases as well as *gauche* alkyl conformations when cholesterol was added [5,33,34].

It should be pointed out that our choice of a random cholesterol distribution among the fatty acids is only one of several possibilities. Chong et al. [35] have suggested a maximum separation of steroid molecules in phosphatidylcholine bilayers. Smondyrev et al. [16] have compared regular cholesterol arrays and cholesterol rich stripes in their MD studies on DPPC/cholesterol mixtures and found differences in equilibration time and stability of the bilayer models. However, we do not have any experimental data concerning an ideal distribution of cholesterol molecules in skin lipids. Thus a random initial distribution was chosen, since we did not want to in-

troduce an artificial order which would obey particular rules, making the results more complex.

5. Conclusions

We have applied MD simulations to obtain a picture of skin lipid model systems on a molecular level. Two models, consisting of hydrated palmitic acid/stearic acid (as representatives of the skin fatty acid fraction) and palmitic acid/stearic acid/cholesterol in equimolar portions, were investigated. The aim of our study was to gain more understanding of the role of cholesterol in SC. From the simulations we obtained a picture of the phase behavior of the fatty acid fraction in the presence and in the absence of cholesterol. The fatty acids stayed at skin temperature in a highly ordered phase, as can be seen directly from the molecular structures and from the *trans* fraction, the area per headgroup, and the order parameters. This is in accordance with numerous investigations, where the results have shown that the SC lipids, in contrast to phospholipid membranes, are not arranged as homogeneous fluid layers, since solid phase domains are present. However, this phase behavior can be smoothed by cholesterol. This well known increase of lipid chain mobility at temperatures below the chain melting transition is adequately reproduced by our simulations: the *trans* fraction and order parameters are decreased and the hydrophobic thickness is reduced. Our MD analysis demonstrates how cholesterol introduces a large number of *gauche* conformers in the fatty acids: the alkyl chains show a strong decrease in conformational order of those atoms adjacent to the cholesterol tails. The parameters which can be calculated from the theoretical work are in good qualitative agreement with the experimental results. The results of this study provide the confidence to extend our SC lipid model for further MD studies on the role of ceramides.

References

[1] P.W. Wertz, B. van den Bergh, The physical, chemical and functional properties of lipids in the skin and other biological barriers, Chem. Phys. Lipids 91 (1998) 85–96.
[2] S.E. Friberg, D.W. Osborne, Small-angle X-ray diffraction patterns of stratum corneum and a model structure for its lipids, J. Dispers. Sci. Technol. 6 (1985) 485–495.
[3] J.A. Bouwstra, G.S. Gooris, M.A. de Vries, J.A. van der Spek, W. Bras, Structure of human stratum corneum as a function of temperature and hydration: a wide-angle X-ray diffraction study, Int. J. Pharm. 84 (1992) 205–216.
[4] D.C. Swartzendruber, P.W. Wertz, D.J. Kitko, K.C. Madison, D.T. Downing, Molecular models of intercellular lipid lamellae in mammalian stratum corneum, J. Invest. Dermatol. 92 (1989) 251–257.
[5] B. Ongpipattanakul, M.L. Francoeur, R.O. Potts, Polymorphism in stratum corneum lipids, Biochim. Biophys. Acta 1190 (1994) 115–122.
[6] N. Kitson, J. Thewalt, M. Lafleur, M. Bloom, A model membrane approach to the epidermal permeability barrier, Biochemistry 33 (1994) 6707–6715.
[7] E. Sparr, K. Ekelund, J. Engblom, S. Engström, H. Wennerström, An AFM study of lipid monolayers. 2. Effect of cholesterol on fatty acids, Langmuir 15 (1999) 6950–6955.
[8] K.M. Merz, B. Roux, Biological Membranes: A Molecular Perspective from Computation and Experiment, Birkhäuser, Boston, MA, 1996.
[9] D.P. Tieleman, S.J. Marrink, H.J.C. Berendsen, A computer perspective of membranes: molecular dynamics studies of lipid bilayer systems, Biochim. Biophys. Acta 1331 (1997) 235–270.
[10] D.J. Tobias, K. Tu, M.L. Klein, Atomic-scale molecular dynamics simulations of lipids, Curr. Opin. Colloid Interface Sci. 2 (1997) 15–26.
[11] E. Egberts, H.J.C. Berendsen, Molecular dynamics simulation of a smectic liquid crystal with atomic detail, J. Chem. Phys. 89 (1988) 3718–3732.
[12] T. Fukada, S. Okazaki, I. Okada, Molecular dynamics study of the lauryl alcohol-laurate model bilayer, Biophys. J. 64 (1993) 1344–1353.
[13] A.J. Robinson, W.G. Richards, P.J. Thomas, M.M. Hann, Behavior of cholesterol and its effect on head group and chain conformations in lipid bilayers: a molecular dynamics study, Biophys. J. 68 (1995) 164–170.
[14] R.R. Gabdoulline, G. Vanderkooi, C. Zheng, Comparison of the structures of dimyristoylphosphatidylcholine in the presence and absence of cholesterol by molecular dynamics simulations, J. Phys. Chem. 100 (1996) 15942–15946.
[15] K. Tu, M.L. Klein, D.J. Tobias, Constant-pressure molecular dynamics investigation of cholesterol effects in a dipalmitoylphosphatidylcholine bilayer, Biophys. J. 75 (1998) 2147–2156.
[16] A.M. Smondyrev, M.L. Berkowitz, Structure of dipalmitoylphosphatidylcholine/cholesterol bilayer at low and high cholesterol concentrations: molecular dynamics simulation, Biophys. J. 77 (1999) 2075–2089.
[17] M. Pasenkiewicz-Gierula, T. Rog, K. Kitamura, A. Kusumi, Cholesterol effects on the phosphatidylcholine bilayer polar region: a molecular simulation study, Biophys. J. 78 (2000) 1376–1389.

[18] M. Goto, E. Asada, The crystal structure of the B-form of stearic acid, Bull. Chem. Soc. Japan 51 (1978) 2456–2459.
[19] R.R. Warner, M.C. Myers, D.A. Taylor, Electron probe analysis of human skin: determination of the water concentration profile, J. Invest. Dermatol. 90 (1988) 218–224.
[20] W.F. van Gunsteren, H.J.C. Berendsen, Groningen Molecular Simulation (GROMOS) Library Manual (1987), Biomos, Groningen.
[21] J.P. Ryckaert, A. Bellemans, Molecular dynamics of liquid alkanes, Faraday Discuss. Chem. Soc. 66 (1978) 95–106.
[22] S. Miyamoto, P.A. Kollman, SETTLE: an analytical version of the SHAKE and RATTLE algorithm for rigid water models, J. Comp. Chem. 13 (1992) 952–962.
[23] R. Lieckfeldt, J. Villalaín, J.-C. Gómez-Fernández, G. Lee, Apparent pK_a of the fatty acids within ordered mixtures of model human stratum corneum lipids, Pharm. Res. 12 (1995) 1614–1617.
[24] D. van der Spoel, A.R. van Buuren, E. Apol, P.J. Meulenhoff, D.P. Tieleman, A.L.T.M. Sijbers, R. van Drunen, H.J.C. Berendsen, Gromacs User Manual, Version 1.6, Biomos, Groningen, 1996, http://rugmd0.chem.rug.nl/–gmx.
[25] R. Mendelsohn, M.A. Davies, J.W. Brauner, H.F. Schuster, R.A. Dluhy, Quantitative determination of conformational disorder in the acyl chains of phospholipid bilayers by infrared spectroscopy, Biochemistry 28 (1989) 8934–8939.
[26] J. Seelig, A. Seelig, Lipid conformations in model membranes and biological membranes, Q. Rev. Biophys. 13 (1980) 19–61.
[27] D.A. Pink, T.J. Green, D. Chapman, Raman scattering in bilayers of saturated phosphatidylcholines. Experiment and theory, Biochemistry 19 (1980) 349–356.
[28] P.A. Hyslop, B. Morel, R.D. Sauerheber, Organization and interaction of cholesterol and phosphatidylcholine in model bilayer membranes, Biochemistry 29 (1990) 1025–1038.
[29] N. Boden, S.A. Jones, F. Sixl, On the use of deuterium nuclear magnetic resonance as a probe of chain packing in lipid bilayers, Biochemistry 30 (1991) 2146–2155.
[30] P. Huang, J.J. Perez, G.H. Loew, Molecular dynamics simulations of phospholipid bilayers, J. Biomol. Struct. Dyn. 11 (1994) 927–956.
[31] M. Gniadecka, O.F. Nielsen, D.H. Christensen, H.C. Wulf, Structure of water, proteins and lipids in intact human skin, hair and nails, J. Invest. Dermatol. 110 (1998) 393–398.
[32] L. Gay, R.H. Golden, V.H.W. Mak, M.L. Francoeur, Characterization of low-temperature lipid transitions in human stratum corneum, J. Invest. Dermatol. 103 (1994) 233–239.
[33] R. Neubert, W. Rettig, S. Wartewig, M. Wegener, A. Wienhold, Structure of stratum corneum lipids characterized by FT-Raman spectroscopy and DSC. 2. Mixtures of ceramides and saturated fatty acids, Chem. Phys. Lipids 89 (1997) 3–14.
[34] G.S.K. Pilgram, A.M. Engelsma-van Pelt, G.T. Oostergetel, H.K. Koerten, J.A. Bouwstra, Study on the lipid organization of stratum corneum lipid models by (cryo-)electron diffraction, J. Lipid Res. 39 (1998) 1669–1676.
[35] P.L.G. Chong, Evidence for regular distribution of sterols in liquid crystalline phosphatidylcholine bilayers, Proc. Natl. Acad. Sci. USA 91 (1994) 10069–10073.